Cold ^{52}Cr elastic and inelastic collision-rate determination using evaporative cooling analysis

Scott V. Nguyen, Robert deCarvalho, and John M. Doyle
Department of Physics, Harvard University, Cambridge, Massachusetts 02138, USA
(Received 23 January 2007; published 15 June 2007)

Elastic and inelastic collision-rate constants of ^{52}Cr in the temperature range of 20 mK to 1 K are inferred from the evaporative cooling of buffer gas loaded atomic chromium. Using a model that describes the dynamics of the trapped chromium cloud during evaporation, we find $g_{\mathrm{el}}=2.15(+2.5,-1.2)\times10^{-10}$ cm^3/s and $g_{\mathrm{in}}=1.36(+1.2,-0.7)\times10^{-12}$ cm^3/s, consistent with theory but in disagreement with previously reported measurements.

DOI: 10.1103/PhysRevA.75.062706 PACS number(s): 32.80.Cy, 31.15.Bs, 32.80.Pj

I. INTRODUCTION

The long-range anisotropic interactions of dipolar gases have generated much interest recently, with theoretical predictions of exotic ground states and novel quantum phase transitions [1–5]. The realization of Bose-Einstein condensation in a cloud of chromium ^{52}Cr [6] now provides an experimental test-bed for the study of these dipolar gases in regimes previously inaccessible by BECs of alkali metals, metastable helium, or ytterbium. The large $6\mu_B$ magnetic moment of the $^7S_3$ groundstate of ^{52}Cr gives rise to a magnetic dipole-dipole interaction 36 times stronger than that in the alkali metals. By tuning the *s*-wave scattering length to zero via a Feshbach resonance [7], it may be possible to create quantum degenerate gases dominated not by the contact interaction but rather by the dipole-dipole interaction.

However, the $6\mu_B$ magnetic moment also leads to high dipolar relaxation rates [8–11]. Trap loss and heating from spin flips due to dipolar relaxation prevented the successful evaporation of ^{52}Cr to quantum degeneracy in a magnetic trap [6,12]. Degeneracy was achieved only after transferring the atoms into an optical trap and optically pumping the atoms into their lowest Zeeman state which is impervious to spin flips. The number of atoms in the BEC is limited by the high atom loss incurred during the initial evaporation of the trap sample down to temperatures cold enough where atoms can be loaded into the optical trap. In the *s*-wave regime, measurements of dipolar relaxation at low magnetic fields for binary collisions between two atoms in state $|S=3,m_S=+3\rangle$ yielded typical rate constants of $g_{\mathrm{DR}}=4\times10^{-12}$ cm^3/s [8], ~3 orders of magnitude larger than that for the alkali metals [13].

Earlier measurements of the dipolar relaxation rate were made at higher temperatures and magnetic fields using a buffer gas loaded sample [10,11]; ^{52}Cr was magnetically trapped at initial temperatures of ~1 K, and then evaporatively cooled. Unfortunately, evaporation stalled at 2 mK. The stated inelastic collision-rate constant in that work increased four orders of magnitude from 10^{-13} to 10^{-9} cm^3/s as the sample was cooled from 1 K down to 5 mK, eventually becoming larger than the measured elastic collision-rate constant of 10^{-11} cm^3/s. The two-body loss was attributed to dipolar relaxation because the sample was spin polarized. The possibility of shape resonances was also suggested as an explanation for the sharp increase in the inelastic rate [11]. Both the measured elastic and dipolar relaxation rates in this temperature range, however, disagree with recent theoretical calculations taking into account all significant partial waves [9,14]. The theoretical values are based on scattering calculations between ^{52}Cr atoms in $|S_{1,2}=3,m_{S1,2}\rangle$ and uses the most accurate to date molecular potential, constructed from the experimental identification of a series of measured magnetic Feshbach resonances in an ultracold sample of chromium atoms [7]. The calculations are also consistent with the dipolar relaxation rates measured in the ultracold regime (<1 mK) [8].

In this paper, we use an evaporative cooling model to extract elastic and inelastic rates from the experimental data of Refs. [10,11]. The evaporative cooling dynamics analysis we perform here produces rate constants that are inconsistent with previous determined values [11] and are consistent with recent theoretical determinations [9,14].

II. MEASURED COLLISION RATES

Figure 1 shows the previously reported elastic g_{el} and inelastic collision-rate constants g_{in} for binary collisions between two atoms in state $|S=3,m_S=+3\rangle$ as a function of temperature [10,11]. Also plotted are the theoretically calcu-

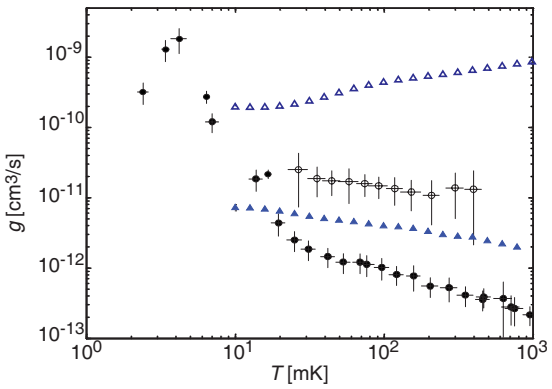

FIG. 1. (Color online) Measured and theoretical collision-rate constants between two $|S_{1,2}=3,m_{S1,2}=+3\rangle$ chromium atoms. The open (solid) circles are the measured elastic (inelastic) rate constants. The open (solid) triangles are the theoretical elastic (inelastic) rate constants. The measured rate constants are taken from Ref. [11]. The theoretical rate constants are taken from Refs. [9,14].

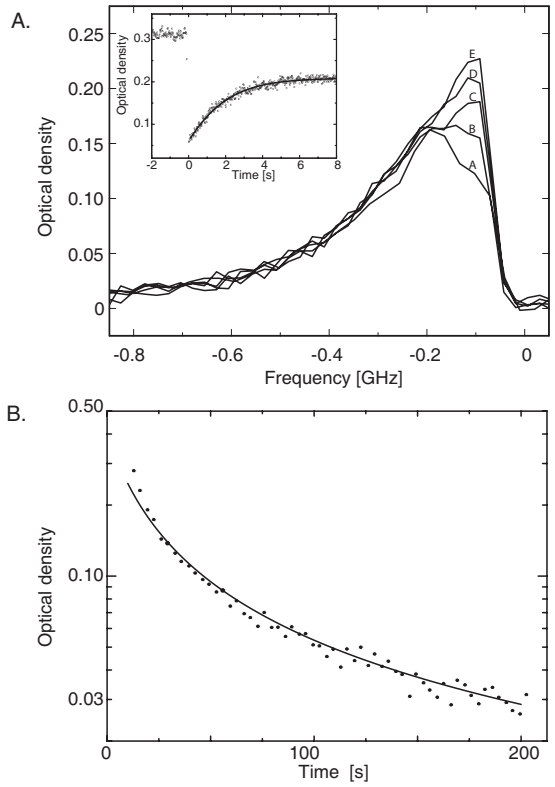

FIG. 2. Experimental methods in which the measured collision-rate constants were extracted. (A) Elastic collision rate. Spectra taken after optically pumping atoms out of the trap, showing a return to a thermal distribution due to elastic collisions. Successive spectra (A)–(E) were taken at 1 s intervals following the optical pumping. The pump beam was tuned to −0.12 GHz. (B) Inelastic collision rate. Trap loss fit to the expected functional form for two-body loss. Graphs were taken from Ref. [17].

lated rate constants by Pavloic *et al.* [9,14]. The discrepancy between measured and theoretical rate constants is dramatic both in value and functional form.

The reported collision-rate constants were obtained by first magnetically trapping ^{52}Cr atoms at ~1 K and then evaporatively cooling the sample to lower temperatures by uniformly lowering the depth of the magnetic trap. The sample was cooled by both adiabatic expansion and forced evaporation. At the colder temperatures, the elastic collision rate was measured by selectively optically pumping atoms out of one part of the thermal distribution and observing the reequilibration of the atomic cloud as shown in Fig. 2(a). The rate at which the cloud returns to a thermal distribution is proportional to the elastic collision rate. The inelastic collision-rate constant was measured by observing trap loss at a constant trap depth. Because the decay of the spin-polarized sample fit well to the expected functional form for two-body loss, trap loss was attributed to Cr-Cr collision induced dipolar relaxation [Fig. 2(b)].

In addition, after the trap depth was lowered to a set value and the atoms were evaporatively cooled, the temperature of the sample was observed to remain constant within the signal to noise of the experiment. The measured temperature was assumed to be the steady-state temperature T_{SS} set by the ratio g_{el}/g_{in} [15]. Figure 3 shows the measured $\eta \equiv E_{th}/k_B T$ as a function of temperature where E_{th} is the depth of the magnetic trap. The decrease in η at colder temperatures is consistent with the measured decrease in the ratio g_{el}/g_{in}.

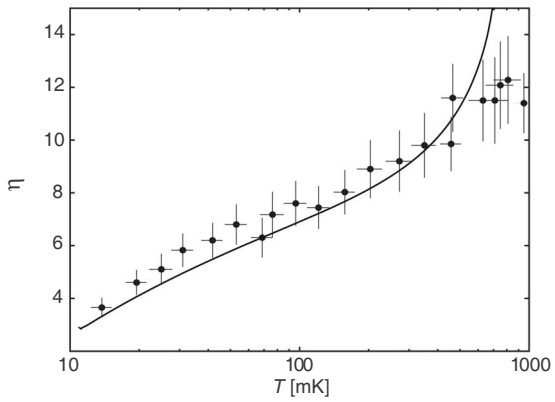

FIG. 3. Measured η as a function of temperature. The solid circles are the measured η after the sample has been evaporatively cooled to a trap depth E_{th}. Data taken from Ref. [17]. The solid line is the η that would be measured predicted by the evaporation model using the the fitted values for the collision rates $g_{el}=2.15\times10^{-10}$ cm^3/s and $g_{in}=1.36\times10^{-12}$ cm^3/s.

III. EVAPORATION MODEL

Motivated by the discrepancy between theory and experiment, we model evaporation with the aim of better understanding the relationship of elastic and inelastic collisions to the properties of the trapped ^{52}Cr sample. The model, which is an extension of the model developed by Doyle *et al.* [16] for the evaporation of atomic hydrogen, consists of two coupled differential equations accounting for the changes in the atom number N and the energy E of the trap distribution due to the various cooling, heating, and loss processes of evaporation.

During evaporation, we consider trap loss due to the following processes.

(1) Evaporation over the trap edge due to elastic collisions at a rate $\dot{N}_{ev}(\eta, g_{el})$. These collisions lead to cooling as higher energy atoms are most likely to be knocked over the trap edge.

(2) Spin flips from magnetically trapped states to untrapped states due to inelastic collisions at a rate $\dot{N}_{in}(\eta, g_{in})$. This leads to heating as inelastic collisions are most likely to occur at the center of the trap.

(3) Atoms lost due to forced evaporation at a rate $\dot{N}_f(\eta)$. This is the fraction of atoms in the high energy tail of the trapped distribution that is above the trap depth.

The combination of all these processes govern the evolution of the number of atoms N in the trap given by the following rate equation:

$$\dot{N} = \dot{N}_{ev} + \dot{N}_{in} + \dot{N}_f. \quad (1)$$

We do not include atom loss due to background gas collisions, three-body recombination, or Majorana flops due to

the zero of quadrupole trap. For the particular experimental parameters in which the collision rates were taken, the rate of these processes were slow compared to the measured evaporation rate and inelastic collision rate. The experiment was performed in a cryogenic environment with an exponential lifetime set by background gas collisions estimated at >200 s. The peak densities were always below 10^{12} cm^{-3}, and the cloud size was always >5 mm. These processes can easily be included by adding the appropriate loss term to Eq. (1). Each $\dot{N}$ term is determined by integrating the loss rate over the volume of the trap. The evaluation of each term for a spherically symmetric trap is presented in Ref. [15]. These terms are valid for all values of η.

For each atom that is lost, there is also a corresponding change in the energy of the trapped distribution $\dot{E}=E\dot{N}$, where E is the energy of the lost atom. When expressed in terms of the average energy $\bar{E}$, each process changes the energy of the trapped distribution according to

$$N\dot{\bar{E}} = (E_{\rm ev} - \bar{E})\dot{N}_{\rm ev} + (E_{\rm in} - \bar{E})\dot{N}_{\rm in} + (E_f - \bar{E})\dot{N}_f + E_{\rm ad}, \quad (2)$$

where we also include the energy change due to adiabatic expansion or compression of the magnetic trap $\dot{E}_{\rm ad}$. Evident from Eq. (2), each loss process can be a heating (cooling) term depending on if the energy of the lost atom is smaller (larger) than the average energy. The evaluation of each energy term is also presented in Ref. [15].

Equations (1) and (2) together provides us a description for the dynamical evolution of the trap distribution during the evaporation process. We solve Eqs. (1) and (2) $N(t)$ and $T(t)$ by inputting the initial conditions and the time profile of the changes in the trap depth $E_{\rm th}$, where T is the temperature of the trapped distribution which is related to $\bar{E}$ by Eqs. (29) and (55) in Ref. [15]. By keeping track of $\dot{N}_{\rm ev}$ and $\dot{N}_{\rm in}$, we can also account for the relative contributions of elastic and inelastic collisions on $N(t)$ and $T(t)$.

IV. EVAPORATION DYNAMICS

In the experiment, 6×10^{11} Cr atoms were initially loaded into a $E_{\rm th}=9$ K deep magnetic trap at a temperature of $T=700$ mK. The magnetic trap depth was then uniformly lowered at an exponential rate of $\tau=4$ s. The 4 s time constant was set by the L/R time of the inductance of the superconducting magnet and the resistor bank circuit through which the current was discharged. Once the trap depth reached a predetermined value, the trap depth was held constant. At this trap depth, the temperature of the cloud and the elastic and inelastic collision rates were measured as described in Sec. II. The measurements were repeated at lower and lower final trap depths.

Figure 4 shows the evaporation dynamics for the specified experimental parameters predicted by the evaporation model. The average measured values of $g_{\rm el}=10^{-11}$ cm^3/s and $g_{\rm in}=10^{-13}$ cm^3/s are used for the elastic and inelastic collision rates. The final trap depth is $E_{\rm th}=0.16$ K. From the simulations, we see that the fast decrease in trap depth quickly leads to a low density of $n_0\sim10^{10}$ cm^{-3}. The single atom collision

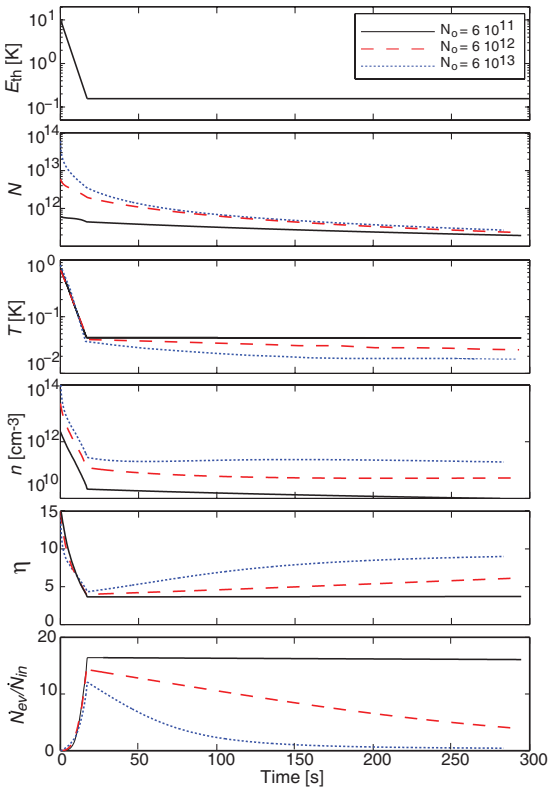

FIG. 4. (Color online) Evaporation dynamics of magnetically trapped Cr. The elastic and inelastic rate constants are $g_{\rm el}=10^{11}$ cm^3/s and $g_{\rm in}=10^{-13}$ cm^3/s ($\eta_{\rm eq}=9.2$). The trap depth varies as $E_{\rm th}=E_0e^{-t/\tau}$, where $E_0=9$ K and $\tau=4$ s. The final trap depth is $E_{\rm th}=0.16$ K.

time at this density is on the order of 10 s. Only a few collisions are necessary to attain internal equilibrium within the gas. However, the balance of elastic and inelastic collisions within the gas, which drive the sample to its steady-state temperature, takes much longer to achieve. This time is indicated as 300 s by the simulations, about 30 times longer than the internal thermal equilibrium time. Only with larger initial atom number and corresponding higher collision rates would allow the system cool to $T_{\rm SS}=17$ mK ($\eta_{\rm eq}=9.2$) within the 300 s window. Therefore, the temperatures that are measured in the experiments at these final trap depths are not typically the steady-state temperature $T_{\rm SS}$. The system has not reached the $\eta_{\rm eq}$ set by the ratio $g_{\rm el}/g_{\rm in}$ within the measurement period. The time scale to reach equilibrium should approximately follow $[n_0 f(\eta) g_{\rm el}]^{-1}$, where $f(\eta)$ is the fraction of elastic collisions resulting in an evaporated atom [13,15]. Low signal-to-noise resulting from the low densities would have prevent experimentally observing any change in temperature over a reasonable timescale as the system approached $T_{\rm SS}$.

As the trap depth is lowered, the η of the trapped distribution is continually decreasing, reflecting the fact that $E_{\rm th}$ is being lowered too quickly for the system to cool to $T_{\rm SS}$. The solid line in Fig. 3 is the η that would be measured after the the system has been evaporatively cooled to a trap depth $E_{\rm th}$. The elastic and inelastic rate constants that are used in the simulation are $g_{\rm el}=2.15\times10^{-10}$ cm^3/s and $g_{\rm in}=1.36$

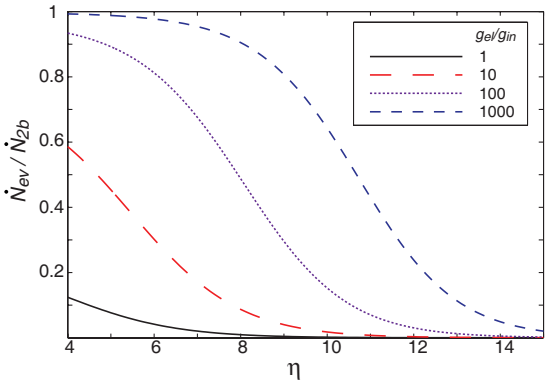

FIG. 5. (Color online) Fraction of two-body loss due to evaporation over the trap edge.

$\times 10^{-12}$ cm^3/s ($\eta_{eq}=10$), values which are inferred from Sec. V. Not only does the curve reproduce the functional form of the measured η, the values are within the error bars. This confirms that the measured values for η are not necessarily η_{eq}. The measured decrease in η as the temperature of the distribution was lowered is an artifact of evaporation procedure and is not a reflection of a decreasing ratio of g_{el}/g_{in}.

In addition, at the low η's reached in the experiment, atom loss is actually dominated by $\dot{N}_{ev}$ rather than $\dot{N}_{in}$ (Fig. 4). For $N_0=6\times10^{11}$ atoms, there is ~16 atoms lost due to evaporation over the trap edge for every one atom lost due to inelastic collisions during the period in which the two-body measurements were taken. Therefore, attributing the two-body decay solely to inelastic collisions is not accurate. According to Eq. (63) in Ref. [15] for a constant trap depth, the measured two-body decay constant is equal to $g_{2b}=f(\eta)g_{el}+g_{in}$. Figure 5 shows the fraction of two-body loss which is due to evaporation over the trap edge for various ratios of g_{el}/g_{in}. Because we have both the measured elastic rate constant and η at the temperature at which the two-body measurements were taken, correcting the reported inelastic rate is possible. However, as we argue in the next section, the measurements of the elastic rate constant may also be misinterpreted.

V. INFERRED ELASTIC AND INELASTIC COLLISION RATES

The analysis based on the simulations thus far has not involved the elastic collision-rate constant. Because of the discrepancy with the theoretical values, the misinterpretation of the inelastic data casts some doubt on the elastic rate measurements. Modifications to the elastic collision-rate measurements would also affect the value of the inelastic rates deduced by the two-body measurements. Therefore resolving the discrepancy between theory and experiment requires a experimental method which is not based on the previous measurement of g_{el} and g_{in}.

Fortunately, data for this independent method already exists. In evaporatively cooling chromium, both the temperature and number of chromium atoms are measured as a function of the trap depth [17]. Since $\dot{N}$ and $\dot{T}$ are both functions

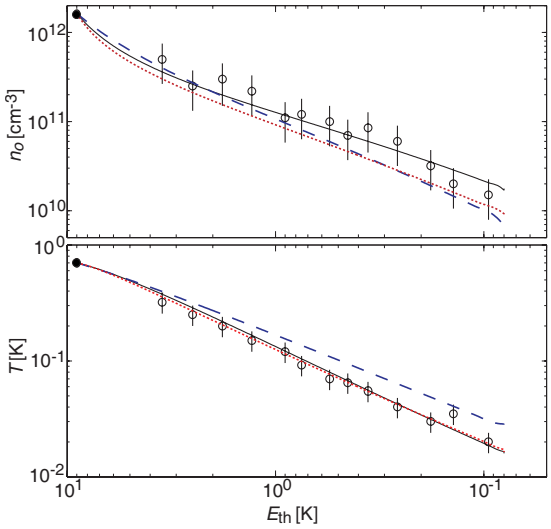

FIG. 6. (Color online) Least-squares fit to the Cr evaporation data. The solid circles are the initial conditions. The open circles are the measured values for n_0 and T after being evaporatively cooled to E_{th}. The solid line is a least squares fit for the elastic and inelastic collision rates yielding $g_{el}=2.15\times10^{-10}$ cm^3/s and $g_{in}=1.36\times10^{-12}$ cm^3/s. The dotted line is evaporation using the theoretically predicted values. The dashed line is evaporation using the average of the experimentally measured values.

of g_{el} and g_{in}, the dynamical evolution of $N(t)$ and $T(t)$ is solely determined by the collision-rate constants and the experimental trap parameters. Therefore we are able to use the evaporation model along with the evaporative cooling data to independently infer elastic and inelastic collision-rate constants.

Figure 6 plots the measured density and temperature after being evaporatively cooled to various final trap depths. At the initial trap depth of 9 K, $n_0=1.8\times10^{12}$ cm^{-3} and $T_0=700$ mK. The trap depth was then lowered exponentially with a time constant of $\tau=4$ s. By numerically solving Eqs. (1) and (2) for n_0 and T as a function of the varying trap depth, we can perform a least squares fit for the values of g_{el} and g_{in} which would best reproduce the measured evaporation data. In this analysis we assume that both g_{el} and g_{in} are constant through the 20 mK–1 K temperature range. Even though there may be some functional dependence on temperature, the theoretical collision rates show only a weak dependence, changing by a factor of ~3 through this temperature range.

A least-squares fit for the data presented in Fig. 6 with g_{el} and g_{in} as fit parameters yields collision rates of $g_{el}=2.15(+2.5,-1.2)\times10^{-10}$ cm^3/s and $g_{in}=1.36(+1.2,-0.7)\times10^{-12}$ cm^3/s with $\chi^2_{fit}=8.1$. If we use the theoretically predicted values for g_{el} and g_{in} which includes the temperature dependence $\chi^2_{theory}=10.7$. Using the average earlier experimentally measured values $g_{el}=1.5\times10^{-11}$ cm^3/s and $g_{in}=7\times10^{-13}$ cm^3/s, $\chi^2_{exp}=66.3$.

The result which stands out the most from this analysis is the elastic collision-rate constant. The fitted value for g_{el} is more than an order of magnitude larger than the measured value and agrees with theoretically predicted values. As seen in Fig. 6, g_{el} must be of this magnitude to account for the

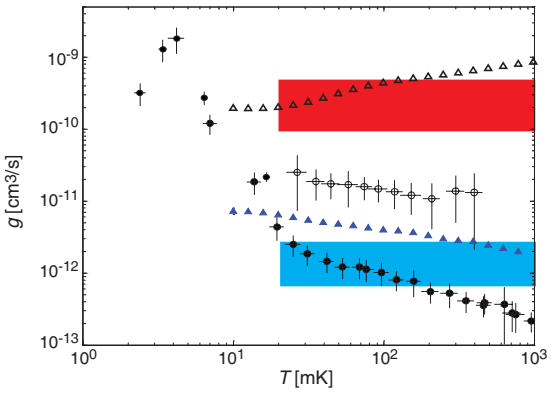

FIG. 7. (Color online) Inferred chromium collision rates. The darker (lighter) shaded region represents the inferred elastic (inelastic) collision rate from a fit of the evaporation data show in Fig. 6. The solid (open) circles are the measured two-body loss (elastic) rates. The solid (open) triangles are the theoretical inelastic (elastic) rates.

amount of cooling that was experimentally measured. With g_{el} tens times slower, cooling due to the evaporation rate over the trap edge is too slow compared to the rate at which the trap depth is lowered.

The fitted value for g_{in} is slightly lower than the theoretically predicted values. It is important to note that the theoretical values presented here have been thermally averaged over the distribution of collision energies, however, it has not been averaged over the distribution of magnetic fields. The theoretical values are the inelastic rate constants at a magnetic field $3B_{max}/2\eta$, which is the magnetic field at which a two-body collision is most likely to occur. Comparing the fitted value for g_{in} to the experimentally measured value is uninformative because the experimental values are dependent on knowing the elastic collision rates. The inferred value of g_{el} now puts into question the analysis of the elastic collision-rate measurements.

VI. CONCLUSIONS

Figure 7 shows a summary of the inferred collision-rate constants based on the evaporation model compared to the theoretical and previously measured rates constants. In the current analysis, the fit to the evaporation data assumes a constant collision rate through this temperature range. However, the analysis can be easily extended to include a temperature dependence if a functional form is known. By comparing the resulting χ^2, we can determine if a particular model better describes the evaporation data. In addition, because reliable evaporation data was only taken for temperatures above 20 mK, the inferred rates are only valid for the temperature range between 20 mK and 1 K. Even though we cannot say with certainty, the large two-body rates ($>10^{-10}$ cm^3/s) that were measured below 20 mK are likely due to a combination of dipolar relaxation and evaporation over the trap edge, which now can be accounted for by both the elastic collision rate and low η at which the measurements were performed.

The reason for the discrepancy between the inferred elastic rate constant and the earlier experimentally measured values remains a mystery. From the evaporation model, we have a good understanding of how to determine the inelastic collision rate. Unfortunately, extracting this value from two-body measurements requires knowing the elastic collision rates. The optical-pumping experiments used to determine the the elastic collision rate relied on measuring the time scale for the atoms to return to a thermal distribution. This time scale is set by a combination of the elastic collision rate, the number of collisions required to repopulate the orbits of the atoms which were optically pumped away, and the density of the particular part of the distribution which would mostly likely repopulate the missing orbits. Reinterpretation or reanalysis of this data is necessary to understand why the elastic collision rate extracted from it is an order of magnitude lower than what is expected.

In addition, further experiments could be conducted to resolve the discrepancy for the collision rates below 20 mK. This could be done by measuring the density and temperature as a function of trap depth and fitting for g_{el} and g_{in} in this region. Another method of determining the collision rates is to measure the two-body loss rate at a given temperature as a function of η since $g_{2b}=g_{in}+f(\eta)g_{el}$. These two methods might avoid any confusion associated with determining the elastic collision rate from optical-pumping experiments.

ACKNOWLEDGMENTS

We would like to thank R. Krems and Z. Pavlovic for their helpful discussion and theoretical calculations of the Cr-Cr collision rates. We also thank J. Weinstein for providing us with the experimental evaporation data and for his insightful comments. This material is based in part upon work supported by the National Science Foundation under Grant Nos. PHY-0457047 and PHY-0071311.

[1] L. Santos, G. V. Shlyapnikov, P. Zoller, and M. Lewenstein, Phys. Rev. Lett. **85**, 1791 (2000).
[2] L. Santos, G. V. Shlyapnikov, and M. Lewenstein, Phys. Rev. Lett. **90**, 250403 (2003).
[3] L. Santos and T. Pfau, Phys. Rev. Lett. **96**, 190404 (2006).
[4] R. Barnett, D. Petrov, M. Lukin, and E. Demler, Phys. Rev. Lett. **96**, 190401 (2006).
[5] A. Micheli, G. K. Brennen, and P. Zoller, Nat. Phys. **2**, 341 (2006).
[6] A. Griesmaier, J. Werner, S. Hensler, J. Stuhler, and T. Pfau, Phys. Rev. Lett. **94**, 160401 (2005).
[7] J. Werner, A. Griesmaier, S. Hensler, J. Stuhler, T. Pfau, A. Simoni, and E. Tiesinga, Phys. Rev. Lett. **94**, 183201 (2005).
[8] S. Hensler, J. Werner, A. Griesmaier, P. O. Schmidt, A. Görl-

itz, T. Pfau, S. Giovanazzi, and K. Rzazewski, Appl. Phys. B **77**, 765 (2003).
[9] Z. Pavlovic, R. V. Krems, R. Cote, and H. R. Sadeghpour, Phys. Rev. A **71**, 061402(R) (2005).
[10] J. D. Weinstein, R. deCarvalho, C. I. Hancox, and J. M. Doyle, Phys. Rev. A **65**, 021604(R) (2002).
[11] R. deCarvalho, C. I. Hancox, and J. M. Doyle, J. Opt. Soc. Am. A **20**, 1131 (2003).
[12] A. Griesmaier, J. Stuhler, and T. Pfau, Appl. Phys. B **82**, 211 (2006).
[13] W. Ketterle and N. J. V. Druten, Adv. At., Mol., Opt. Phys. **37**, 181 (1996).
[14] Z. Pavlovic, B. O. Roos, R. Cote, and H. R. Sadeghpour, Phys. Rev. A **69**, 030701(R) (2004).
[15] R. deCarvalho and J. Doyle, Phys. Rev. A **70**, 053409 (2004).
[16] J. M. Doyle, J. C. Sandberg, I. A. Yu, C. L. Cesar, D. Kleppner, and T. J. Greytak, Physica B **194**, 13 (1994).
[17] J. D. Weinstein, Ph.D. thesis, Harvard University, Cambridge, 2001.